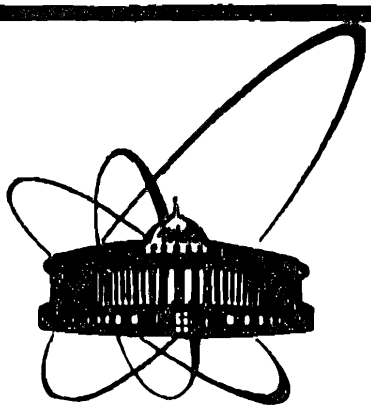

объединенный
институт
ядерных
исследований
дубна

E4-87-409

G.Saupe[1], O.I.Serdiuk[2], G.D.Adeev[2],
V.V.Pashkevich

DESCRIPTION OF THE MASS AND KINETIC-ENERGY DISTRIBUTIONS OF FISSION FRAGMENTS USING AN ADIABATIC POTENTIAL

Submitted to "Ядерная физика"

[1] Zentralinstitut fuer Kernforschung, Rossendorf, GDR
[2] Omsk State University, Omsk, USSR

1987

Introduction

The investigation of the mass and energy distributions of fission fragments in heavy-ion reactions still remains an interesting subject of many experimental and theoretical papers /1-5/. The situation in this field is characterized by the fact that most of the calculations have been performed in the framework of statistical or dynamical approaches, but these models give values of the variances of the mass distributions which are substantially smaller than the measured ones. This disagreement appears for both low and high excitation fission. On the other hand, in the recent yeârs various attempts have been made in order to reproduce the widths of the mass and charge distributions of final fragments from deep-inelastic heavy-ion collisions. For example, Schmidt and Wolschin /6/, who used the stationary solution of a Fokker-Planck equation for the distribution function of the collective variables characterizing the dinuclear system for the calculation of the mass distributions, got a reasonable agreement between the theoretical and the experimental results. Of course, in these calculations the potential energy of the system was approximated by a simple oscillator-like expression which corresponds to the Gaussian shape of the resulting distribution function. In general, many interesting features of deep-inelastic heavy-ion reactions have successfully been explained in terms of this so-called fluctuation-dissipation dynamics /7/. Later this concept has also been applied to the description of the mass and kinetic-energy distributions of fission fragments /8-10/. Recently, in ref. /11/, a calculation based on this formalism for the mass distributions of fission fragments originating from the decay of compound nuclei with a fissility parameter lying in the range $30 < Z^2/A < 40$ has been published. In this paper the investigations have been restricted to the fission of highly excited nuclei where shell and pairing corrections do not play a role. That means that the potential energy can be described in a relatively simple manner and this simplifies considerably the mathematical problems connected with the solution of the corresponding differential equation. In addition, in these calculations the angular momentum of the fissioning nucleus has been taken into account /12/ in calculating the total potential entering into the Fokker-Planck equation. As a consequence, the potential energy surface for the saddle-point configuration changes significantly and the stiffness coefficients become angular-momentum dependent too. It may be expected that the consideration of the rotation of the de-

formed system may lead to a more realistic description of the variances of the fission-fragment mass and energy distributions.
The aim of the present paper is the reproduction of the widths of mass distributions for the fission of composite nuclear systems with fissility parameters $Z^2/A > 40$. At the same time an attempt is being made to reproduce the measured two-dimensional kinetic energy vs. mass plots. The two-body nuclear viscosity coefficient determining the intensity of the dissipation process along the trajectory from the saddle to the scission point is the only free parameter in the diffusion model employed.
The reactions ^{40}Ar (301 MeV) + ^{232}Th and ^{22}Ne (174 MeV) + ^{249}Cf /2/ have been chosen as examples for the present theoretical investigation because in these cases the bombarding energies lie well above the Coulomb and the fission barriers in the entrance channel. From the symmetric shapes of the mass distributions measured in the exit channel of these reactions one can suppose that after the formation of a deformed dinuclear system its further development leads into the usual fission valley. That is why the dynamics involved in the exit channel of such fusion-fission like processes can be described using an adiabatic potential. In the cases under discussion the excitation energies of the composite systems and, consequently, the nuclear temperatures at the saddle points are also so high that shell effects can be neglected so that only the macroscopic liquid-drop term has to be considered.

The model

All the physical and mathematical details of the formalism used here have been discussed in refs. /11,15/. In the present paper the potential energy has been calculated as the adiabatic potential according to Myers and Swiatecki /16/ using the parametrization $\{c, h, \alpha\}$ of the nuclear shape /13/. The parameters c and h describe the elongation and the necking of the system, while the value of α characterizes the left-right asymmetry of the nuclear shape. In the computation for mirror symmetric potentials the trajectories lie in the two-dimensional $\{c, h\}$-space although, in ref. /14/, it has been shown that h = 0 gives the fission path with a good approximation. The collective variables, whose distribution function obeys the Fokker-Planck equation, are the distance R between the future fragment mass centres and the future mass asymmetry which is given by the expression

$X = \frac{A_2 - A_1}{A_1 + A_2}$. Here, A_1 and A_2 are the mass numbers of the two reaction products. The values of R and X are connected with the parameters c and α by the transformation

$$R = \frac{\int_{z_n}^{z_2} z\,\rho^2(z)\,dz}{\int_{z_n}^{z_2} \rho^2(z)\,dz} - \frac{\int_{z_1}^{z_n} z\,\rho^2(z)\,dz}{\int_{z_1}^{z_n} \rho^2(z)\,dz}, \qquad (1)$$

$$X = -\frac{\int_{z_n}^{z_2} \rho^2(z)\,dz}{\int_{z_1}^{z_2} \rho^2(z)\,dz} - \frac{\int_{z_1}^{z_n} \rho^2(z)\,dz}{\int_{z_1}^{z_2} \rho^2(z)\,dz}, \qquad (2)$$

with z and ρ being the usual cylindrical coordinates, where the value of ρ depends on z according to the formula

$$\rho^2 = c^2 R_0^2 \left(A_s + \alpha u + (B - A_s) u^2 - \alpha u^3 - B u^4 \right). \qquad (3)$$

In eq. (3) R_0 refers to the radius of the corresponding spherical nucleus (Z,A), u is given by $u = \frac{z}{c R_0} + \frac{\alpha c^3}{5}$, and A_s is defined as $A_s = c^{-3} - \frac{B}{5}$ with $B = \frac{c - 1}{2} + 2h$. The integration limits are $z_1 = -c R_0 \left(1 + \frac{\alpha c^3}{5}\right)$, $z_2 = c R_0 \left(1 - \frac{\alpha c^3}{5}\right)$, and the neck coordinate z_n which is obtained on condition that $\rho(z)$ reaches it minimum at $z = z_n$.

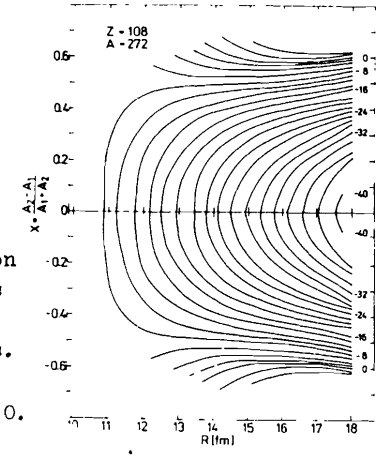

Fig. 1. Contour plot of the deformation energy (in MeV) of the nucleus (Z = 108, A = 272) resulting from the liquid-drop model, vs. the distance R and the mass asymmetry X for h = 0 and l = 0.

Fig. 1 shows the potential landscape for the system (Z = 108, A = 272). It is seen that there is nearly no fission barrier. This is in fact a consequence of the neglect of shell effects which play the most important role for the calculation of the fission barrier in such heavy systems /17/. Including shell corrections Cwiok et al. obtained the value V_B = 7.97 MeV for the barrier of a hypothetical nucleus with (Z = 108, A = 272).

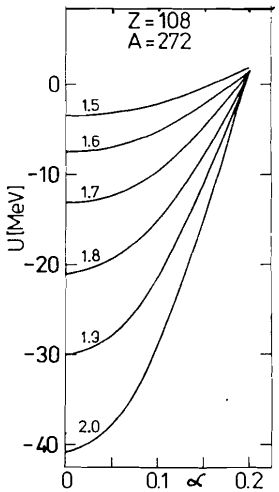

Fig. 2. Dependence of the potential energy of the nucleus (Z = 108, A = 272) for l = 0 on the asymmetry parameter α for different values of the elongation parameter c.

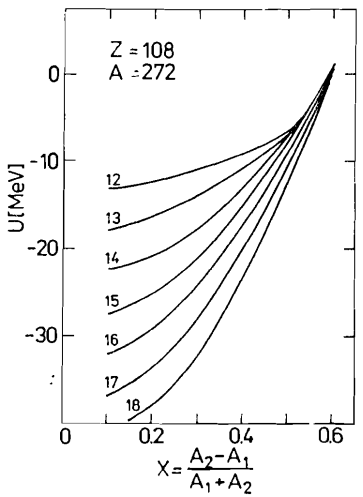

Fig. 3. Dependence of the potential energy of the nucleus (Z = 108, A = 272) for l = 0 on the mass asymmetry X for different values of the distance R (in fm).

Figs. 2 and 3 demonstrate cuts of the potential energy surface along the coordinate α at fixed values of the parameter c and along the coordinate X at fixed values of R. From these two pictures one can conclude that the potential energy U depends on the asymmetry parater at constant values of the elongation nearly quadratically. This allows us to approximate the potential energy by an oscillator potential in order to facilitate the numerical calculations. In the following, the stiffness coefficients for asymmetric variations of the shape have been estimated from analytical approximations for the curves in figs. 2 and 3. The results for $C_\alpha = \left(\frac{\partial^2 U}{\partial \alpha^2}\right)\Big|_c$ and $C_X = \left(\frac{\partial^2 U}{\partial X^2}\right)\Big|_R$ vs. the elongation parameters c and R, respectively,

are represented in fig. 4. Their behaviour is characterized by a sharp increase with approaching the scission point, this being in agreement with the results of other investigations /11,18/.

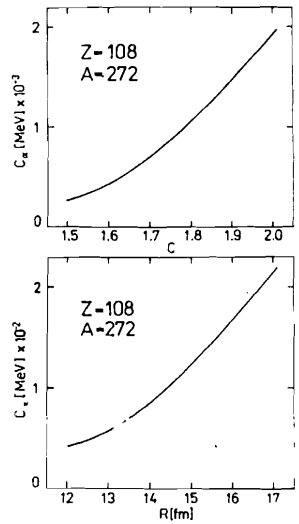

Fig. 4. Dependence of the stiffness coefficients C_α and C_X for l = 0 on the elongation parameters c and R, respectively.

Influence of the angular momentum

Because there is a wide range of the initial angular momentum $0 \leq l_o \leq l_{trap}$ at which fusion-fission processes can take place, the dependence of the variances of the mass and energy distributions on the spin of the composite system has to be considered. In principle, the angular momentum influences the fission process in four ways: (i) the actual excitation energy of the system is lower than the maximum one according to $E_l^* = E_{max}^* - V_{cent}(l_o)$, where the rotational energy is given by $V_{cent}(l_o) = \frac{\hbar^2 l_o^2}{2\mu R_{int}^2}$ /19/ with μ being the reduced mass of the nuclear system in the entrance channel, and R_{int} refers to the interaction radius. (ii) The saddle point shifts to the potential region corresponding to the smaller values of the deformation parameters. (iii) The fission barrier decreases. (iv) The stiffness coefficients increase when the rotational energy is taken into account in the calculation of the total potential energy. In the reactions considered here the first and the second points are expected to be the most important ones because there is almost no fission barrier even for l = 0. In order to obtain an upper limit for the effects mentioned above, the maximum value l_{max} of the angular momentum which can be transferred to the assumed compound nucleus has to be found. In heavy-

ion reactions the value of l_{max} is determined by one of two possible criteria. On the one hand, the entrance channel potential gets a "pocket" for decreasing initial angular momentum so that the projectile is finally trapped. This process leads to a limitation for l_o in the first stage of the reaction. Then, the sticking condition

$$l_{max} = \frac{J_1 + J_2}{\sqrt{\mu(R_1+R_2)^2 + J_1 + J_2}}\, l_{trap} \qquad (4)$$

allows an estimation of the maximum angular momentum transferred to the spin of the fragments. In eq. (4), J_1 and J_2 denote the rigid-body moments of inertia of the projectile and target nuclei whose radii are R_1 and R_2, respectively. On the other hand, the condition of stability against rotation /19/

$$2.1\, A^{-7/3}\, l_{crit}^2 \approx \frac{7}{5}\,(1 - x)^2 \qquad (5)$$

should be fulfilled for the composite system. In the last formula x refers to the fissility parameter. The results of all these estimates are summarized in table 1. In ref. /20/ the critical value of the spin of the compound nucleus which is assumed to be formed in the first reaction has been obtained as $l_{crit} \approx 58\ \hbar$. This is in agreement with the value resulting from the sticking condition. The deviation from l_{crit} calculated here may be explained by the consideration of higher terms in (1 - x) entering in eq. (5) in ref. /20/.

Table 1: Characteristic reaction parameters

System	a	b	c	d	e	f	g	h
$^{40}Ar + {}^{232}Th$	301	105	58	49	30	9.9	119.1	2.1
$^{22}Ne + {}^{249}Cf$	174	71	51	49	30	10.7	87.0	1.8

a) Kinetic energy, E_{lab}, of the projectile (in MeV).
b) Limitation value, l_{trap}, in the entrance channel (in $\hbar$).
c) Transferred angular momentum l_{max} (in $\hbar$).
d) l_{crit} (in $\hbar$).
e) Mean value of the angular momentum $\bar{l}$ (in $\hbar$) of the composite system.
f) Rotational energy, $V_{cent}(\bar{l})$ (in MeV), for the value of $\bar{l}$ from column e.
g) Excitation energy, $E^*(\bar{l})$ (in MeV), for the value of $\bar{l}$ from column e.

h) Temperature of the composite system (Z = 108, A = 272) for the value of $\bar{l}$ from column e.

From table 1 it is seen that in the reactions investigated here the physical limitation for the initial angular momenta leading to fusion-like trajectories is given by the second criterion.
At the end of this section the influence of the angular momentum on the stiffness coefficients is discussed. Taking into account the spin of the composite system, the term

$$E_{rot} = \frac{\hbar^2\, l^2}{2\, J_\perp} - \frac{\hbar^2\, l^2}{2\,\frac{2}{5}\, A\, R_o^2} \qquad (6)$$

is to be added to the deformation energy in order to get the total potential energy. In ref. /13/ the adiabatic moments of inertia parallel and perpendicular to the axis of symmetry have been calculated for symmetric nuclear shapes. Extending this formalism to asymmetric shapes ($\alpha \neq 0$) one gets

$$J_\parallel = \frac{2}{5}\, A\, R_o^2 \left[c^{-1} - \frac{2}{35}\, c^2\,(c-1) + \frac{4}{525}\, c^5\,(c-1)^2 + \frac{1}{7}\,\alpha^2\, c^5 \right] \qquad (7a)$$

$$J_\perp = \frac{1}{2}\, J_\parallel + \frac{1}{5}\, A\, R_o^2 \left[c^2 + \frac{4}{35}\, c^5\,(c-1) - \frac{1}{5}\,\alpha^2\, c^8 \right] . \qquad (7b)$$

These relations lead to the following l-dependence of the stiffness coefficients which is given by the term

$$C_{\alpha,l} = \left(\frac{\partial^2 E_{rot}}{\partial \alpha^2}\right)\Bigg|_c = E_{rot},\ sph \left(\frac{\left(\frac{2}{5}\, A\, R_o^2\right)}{J_\perp(c, \alpha=0)}\right)^2 c^5 \left(\frac{c^3}{5} - \frac{1}{7}\right) . \qquad (8)$$

For l = 50 $\hbar$ the maximum value of $C_{\alpha,l}$ (for c = 2) amounts to 80 MeV. This means that in the extreme case of the largest spin of the deformed nuclear system the value of C_α has to be increased by only 4%. Consequently, one can conclude that the angular momentum dependence of the stiffness coefficients is not important for the description of the dynamics of the fission process. But from the change in the potential energy surface and from the shift of the saddle point in the direction of smaller elongation parameters it follows that the calculation along the fission trajectory starts at smaller values of the stiffness coefficients as indicated also in fig. 4. This fact has been discussed in detail in ref. /12/, where a significant increase in the calculated widths of the mass distributions has been obtained for increasing angular momentum.
In principle, one has to take an average over all possible angular

momenta in the entrance channel contributing to fusion-fission like processes in the reaction considered when calculating the variances of the mass and energy distributions of the fission fragments. But in ref. /12/ it has been shown that the calculation of these widths for the mean value of the angular momenta from 0 up to l_{max} gives a good approximation for the result of the averaging procedure mentioned above.

Results and discussion

Using the parameters from table 1 as input ones for the solution of the Fokker-Planck equation one gets the following results represented in table 2 and figs. 5 and 6.

Table 2: Calculated parameters of the kinetic-energy and mass distributions of the fission fragments and experimental values for the widths of the mass distributions. The $\bar{E}_k^V$ values correspond to the fission systematics given by Viola /24/.

System	T(MeV)	l(ħ)	$\bar{E}_k$(MeV)	$\bar{E}_k^V$(MeV)	$\sigma^2_{E_k}$(MeV^2)	σ^2_M(amu^2)
$^{40}Ar + ^{232}Th$	2.2	0	221.1	215.0	746	1134
	2.1	30	219.0		749	1275
$^{22}Ne + ^{249}Cf$	1.9	0	222.4	215.2	659	1023
	1.8	30	220.6		652	1121

System	$\sigma^2_{M,exp}$(amu^2)
$^{40}Ar + ^{232}Th$	1037 ± 140
$^{22}Ne + ^{249}Cf$	1452 ± 158

Here also should be mentioned that the initial conditions for the first and second moments of the distribution functions for the collective variables and their conjugate momenta have been chosen according to the thermal equilibrium conditions.

Fig. 5 shows the contour plots of the kinetic energy vs. mass distributions for the products from the reaction $^{40}Ar + ^{232}Th$, where the calculations have been performed for two different nuclear temperatures caused by different values of the angular momentum. It is seen that the general features of these plots are in good agreement with those of the measured kinetic energy vs. mass distributions (figs. 7 and 9 in ref. /2/). In addition, fig. 5 demonstrates the increase in

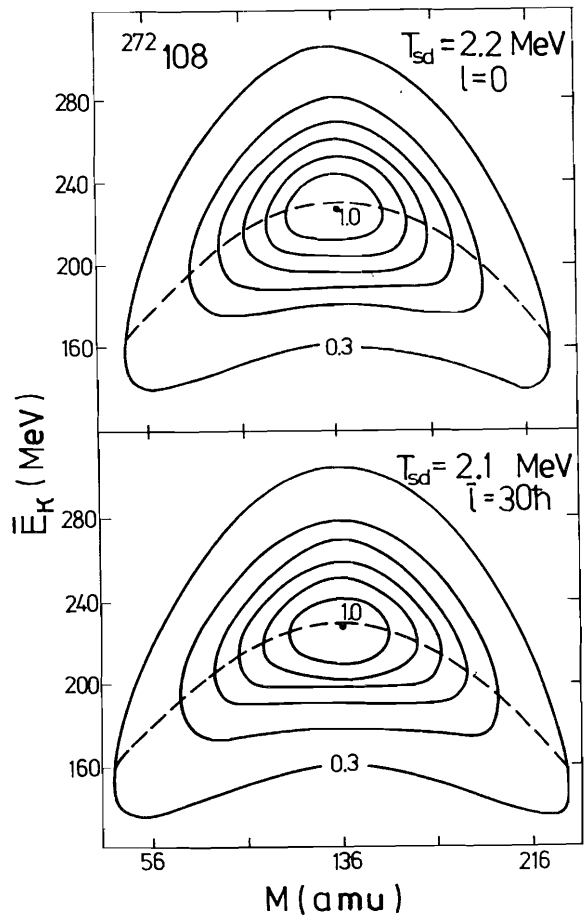

Fig. 5. Kinetic energy vs. mass distributions for the decay of the nuleus (Z = 108, A = 272). The points in the centres of these plots refer to the maxima of the distributions which have been normalized to 1.0. The difference between two contour lines is 0.117 of the maximum value. The dashed lines show the calculated dependences of the mean kinetic energies on the fragment masses.

the width of the fission-fragment mass distribution with increasing angular momentum of the decaying system. But it should be pointed out that the gross properties of such experimentally obtained two-dimensional contour plots are very similar for the fission of a compound nucleus as well as for quasi-fission (see, for example, refs. /21,22/). That is why the character of these diagrams does not allow an unambiguous conclusion about the mechanism of the decay of the rotating system produced in the concrete reaction. In

order to clarify the nature of the reaction process one had to measure the angular distributions of the fission fragments, too.
The computed first and second moments of the energy-mass distributions may also be compared with the experimental findings. Fig. 5 also shows the calculated dependences of the mean kinetic energies $\bar{E}_k(M)$ on the fragment masses. This behaviour of $\bar{E}_k(M)$ can be described in a first approximation by the parabolic expression

$$\bar{E}_k(M) = \bar{E}_k(\tfrac{A}{2}) \left[1 - \beta (1 - \tfrac{2M}{A})^2\right] . \qquad (9)$$

As was found in ref. /23/, the experimental dependence of $\bar{E}_k(M)$ on the mass can be reproduced for the pre-actinides by the factor $\beta < 1$. For the reaction $^{40}Ar + ^{232}Th$, the corresponding values are $\beta = 0.704$ for $l = 0$ and $\beta = 0.644$ for $l = 30\,\hbar$. Besides, the mean values of the kinetic energy distributions (see table 2) obtained for symmetric fragmentation are in good agreement with those of the fission systematics /24/ and with the experimental ones presented in figs. 7 and 9 of ref. /2/. Table 2 gives also the theoretical values of the variances of the mass (σ^2_M) and kinetic energy ($\sigma^2_{E_k}$) distributions which follow from the two-dimensional plots by integration over the other variables. It is seen that the influence of the angular momentum on the calculated characteristics of the distributions is not so strong. A considerable increase in the widths with angular momentum can only be observed in the mass distributions. But also in this case the difference between the results for l=0 and l=I amounts to only 15%.

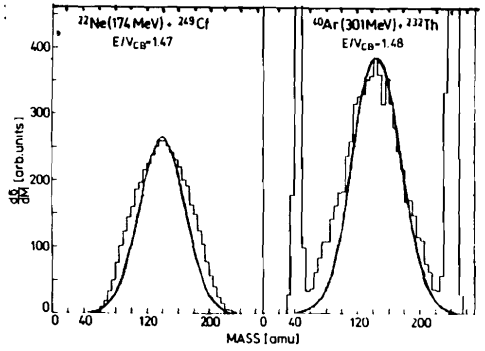

Fig. 6. Experimental (histogram) and theoretical (curve) mass distributions of the fission fragments from the reactions $^{40}Ar + ^{232}Th$ and $^{22}Ne + ^{249}Cf$ at incident energies well above the Coulomb and fission barriers.

Fig. 6 shows a comparison between the calculated Gaussian mass distributions and the measured yields vs. the mass of the reaction products. For the first system considered, the theoretical and the experimental values of σ^2_M are in satisfactory agreement, while for the reaction $^{22}Ne + ^{249}Cf$ the discrepancy is substantial. Of course, on one hand,

it has already been found /11/ that the variances increase with the growth of the fissility parameter Z^2/A. On the other hand, if the fusion-fission process is assumed to take place, it should be expected that the variances increase with increasing excitation energy. If the two systems under discussion are compared with respect to these two parameters, one should suppose a dominance of the second effect because there is a substantially higher excitation energy stored in the system $^{40}Ar + ^{232}Th$, while the difference between the fissility parameters amounts to only ≈ 0.4 %. This argument agrees with the tendency of the theoretical predictions, but the behaviour of the experimental data is characterized by the opposite trend. Especially the large width of the fission fragment mass distribution originating from the reaction $^{22}Ne + ^{249}Cf$ cannot be understood by assuming the usual fusion-fission process. In this case it is possible that another reaction mechanism may manifest itselfs caused by the extremely large mass asymmetry (X = 0.838) in the entrance channel.

Conclusions

The description of the fission-fragment mass distributions in very heavy rotating systems with a fissility parameter $Z^2/A > 40$ in the framework of the diffusion model shows that the influence of the angular momentum on the variances of these distributions is not important. For the reaction $^{40}Ar + ^{232}Th$ the calculated value of the width is in good agreement with the experimental one.
As a next step of these investigations it becomes necessary to perform dynamical calculations for the evolution of the nuclear system in the entrance channel. Thus, if one considers the evolution of the system from the entrance channel to the final decay into two pieces, one should get more realistic trajectories leading to the scission point for each value of the angular momentum l_o contributing to the fragment distributions measured in the exit channel.
The integration over all these contributions with an appropriate weight factor is hoped to give results which are in reasonable agreement with the experimental findings.

References

1. Yu.Ts. Oganessian and Yu.A. Lazarev. Heavy ions and nuclear fission. In: Heavy ion science. Bromley A.D. (ed.), Vol. 4, p. 1, New York, Plenum Press 1984.
2. P.Gippner, K.D.Schilling, W.Seidel et al. Z.Phys., 1986, A325, 335.

3. B.D. Wilkins, E.P. Steinberg, R.R. Chasman. Phys. Rev., 1976, C14, 1832.
4. J.R. Nix. Nucl. Phys., 1969, A130, 241.
5. R.W. Hasse. Nucl. Phys., 1969, A128, 609; Phys. Rev., 1971, C4, 572.
6. R. Schmidt and G. Wolschin. Z. Phys., 1980, A296, 215.
7. H.A. Weidenmueller. Progr. Particle Nucl. Phys., 1980, 3, 49.
8. K. Pomorsky and H.J. Hoffmann. J. Phys. (Paris), 1981, 42, 381.
9. C. Gregoire and F. Scheuter. Z. Phys., 1981, A303, 337.
10. S.K. Samaddar, D. Sperber, M. Zielinska-Pfabe et al. Phys. Scr., 1982, 25, 517.
11. G. D. Adeev and I.I. Gonchar. Z. Phys., 1985, A320, 451.
12. G.D. Adeev, L.A. Marchenko, V.V. Pashkevich et al. JINR P4-86-247, Dubna, 1986.
13. M. Brack, J. Damgaard, H.C. Pauli et al. Rev. Mod. Phys., 1972, 44, 320.
14. C. Gregoire, B. Remaud, C. Ngo. Nucl. Phys., 1982, A383, 392.
15. G.D. Adeev, I.I. Gonchar, L.A. Marchenko et al. Yad. Fiz., 1986, 43, 1137.
16. W.D. Myers and W.J. Swiatecki. Ark. Fys., 1967, 36, 343.
17. S. Cwiok, V.V. Pashkevich, J. Dudek et al. Nucl. Phys., 1983, A410, 254.
18. V.M. Strutinsky. Zh. Eksp. Teor. Fiz. (USSR), 1963, 45, 1900.
19. G. Wolschin. Nucl. Phys., 1979, A316, 146.
20. S. Cohen, F. Plasil, W.J. Swiatecki. Ann. of Phys., 1974, 82, 557.
21. F. Plasil, S.D. Burnett, H.C. Britt et al. Phys. Rev., 1966, 142, 696.
22. R. Bock, Y.T. Chu, M. Dakowski et al. Nucl. Phys., 1982, A388, 334.
23. Ye.I. Gruzintsev, M.G. Itkis, V.N. Okolovich et al. Yad. Fiz., 1984, 39, 1100.
24. V.E. Viola. Nucl. Data, 1966, 1, 391.

Received by Publishing Department
on June 11, 1987.

Саупе Г. и др.

E4-87-409

Описание массового и энергетического распределения
осколков деления на основе адиабатического потенциала

Массовые распределения осколков деления вращающихся ядерных систем с параметром $Z^2/A > 40$ были рассчитаны в рамках диффузионной модели, основанной на уравнении Фоккера — Планка для функции распределения коллективных переменных. В этом подходе единственным свободным параметром является коэффициент двухтельной ядерной вязкости, характеризующий интенсивность диссипативных сил. Показано, что учет углового момента делящегося ядра ведет к небольшому увеличению рассчитанных дисперсий массовых распределений, незначительно улучшая согласие с экспериментальными данными. Кроме того, были также рассчитаны распределения кинетической энергии осколков деления для этих же ядер, которые сравниваются с экспериментальными распределениями.

Работа выполнена в Лаборатории теоретической физики ОИЯИ.

Препринт Объединенного института ядерных исследований. Дубна 1987

Saupe G. et al.

E4-87-409

Description of the Mass and Kinetic-Energy Destributions
of Fission Fragments Using an Adiabatic Potential

The mass distributions of fission fragments from rotating composite nuclear systems with fissility parameters $Z^2/A > 40$ have been calculated in the framework of the diffusion model based on the Fokker-Planck equation for the distribution function of the collective variables. In this formalism the two-body nuclear viscosiry coefficient describing the intensity of the dissipative force is the only free parameter. It has been found that the consideration of the angular momenta of the fissioning nuclei leads to a small increase in the calculated widths which slightly improves the agreement with the experimental data. In addition, the fission fragment kinetic-energy distributions have been calculated and compared with the measured ones.

The investigation has been performed at the Laboratory of Nuclear Physics, JINR.

Preprint of the Joint Institute for Nuclear Research. Dubna 1987